ELSEVIER

Computers & Geosciences 34 (2008) 1223–1242

COMPUTERS & GEOSCIENCES

www.elsevier.com/locate/cageo

Sedtrans05: An improved sediment-transport model for continental shelves and coastal waters with a new algorithm for cohesive sediments ☆

Urs Neumeier[a,*,1], Christian Ferrarin[b], Carl L. Amos[a], Georg Umgiesser[b], Michael Z. Li[c]

[a]*School of Ocean and Earth Science, National Oceanography Centre, University of Southampton, European Way, Southampton SO14 3ZH, UK*

[b]*ISMAR-CNR Venice, Venezia, Italy*

[c]*Geological Survey of Canada, Bedford Institute of Oceanography, P.O. Box 1006, Dartmouth, Nova Scotia, Canada B2Y 4A2*

Received 16 October 2006

Abstract

The one-dimensional (vertical) sediment-transport model SEDTRANS96 has been upgraded to predict more accurately both cohesive and non-cohesive sediment transport. Sedtrans05 computes the bed shear stress for a given set of flow and seabed conditions using combined wave-current bottom boundary layer theory. Sediment transport (bedload and total load) is evaluated using one of five methods. The main modifications to the original version of the model are: (1) a reorganization of the code so that the computation routines can be easily accessed from different user interfaces, or may be called from other programs; (2) the addition of the Van Rijn method to the options for non-cohesive sediment transport; (3) the computation of density and viscosity of water from temperature and salinity inputs; and (4) the addition of a new cohesive sediment algorithm. This latter algorithm introduces variations of sediment properties with depth, represents the suspended sediment as a spectrum of settling velocities (i.e. size classes), includes the flocculation process, and models multiple erosion–deposition cycles. The new model matches slightly better the field measurements of non-cohesive sediment transport, than does the predictions by SEDTRANS96. The sand-transport calibration has been extended to high transport rates. The cohesive sediment algorithm reproduced well experimental data from annular flume experiments.

Keywords: Cohesive sediment transport; Sand transport; Numerical model; Sediment dynamics; Continental shelf; Estuarine processes

1. Introduction

Predicting the transport of non-cohesive (sand) and cohesive (mud) sediments in estuaries and on continental shelves is of great practical importance as these processes can have significant impacts on seabed stability, on the dispersal of particulate material, and on benthic habitat distribution.

☆ Code available from server at http://www.iamg.org/CGEditor/index.htm.

*Corresponding author. Tel.: +1 418 7231986x1278; fax: +1 418 7241842.

E-mail addresses: urs_neumeier@uqar.qc.ca (U. Neumeier), c.ferrarin@ismar.cnr.it (C. Ferrarin), cla8@noc.soton.ac.uk (C.L. Amos), georg.umgiesser@ismar.cnr.it (G. Umgiesser), mli@nrcan.gc.ca (M.Z. Li).

[1]Present address: Institut des sciences de la mer de Rimouski, Université du Québec à Rimouski, 310 allée des Ursulines, Rimouski, QC, Canada G5L 1G3.

0098-3004/$ - see front matter © 2008 Elsevier Ltd. All rights reserved.
doi:10.1016/j.cageo.2008.02.007

Nomenclature

A_{ulva}	bed fraction covered by vegetation
C_0	initial SSC ($kg\,m^{-3}$)
C_{dr}	constant for the drag reduction formula ($m^3\,kg^{-1}$)
C_{solid}	coefficient for the solid-transmitted stress by free-moving vegetation
C_t	SSC after time t ($kg\,m^{-3}$)
$C_{(i)}$	SSC of each W_s class ($kg\,m^{-3}$)
D	(median) sediment grain diameter (m)
D_t	constant for turbulent disruption during erosion
D_*	dimensionless grain size
E_0	empirical coefficient for minimum erosion ($kg\,m^{-2}\,s^{-1}$)
F_k	flocculation coefficient
F_m	flocculation coefficient
g	gravity ($m\,s^{-1}$)
h	water depth (m)
H_s	significant wave height (m)
k_{cd}	coefficient for the relationship between τ_{cd} and W_s
m_{cd}	coefficient for the relationship between τ_{cd} and W_s
m_o	dry mass of overlaying sediment ($kg\,m^{-2}$)
P_e	proportionality coefficient for erosion ($Pa^{-0.5}$)
P_s	probability coefficient of resuspension
q	bedload transport rate ($m^2\,s^{-1}$)
r_d	deposition rate of cohesive sediment ($kg\,m^{-2}\,s^{-1}$)
r_e	erosion rate of cohesive sediment ($kg\,m^{-2}\,s^{-1}$)
S	salinity (practical salinity scale)
SSC	suspended sediment concentration ($kg\,m^{-3}$)
t, Δt	time, time interval (s)
u_{*crs}	critical shear velocity for sediment suspension ($m\,s^{-1}$)
T	temperature (°C)
T_m	dimensionless shear stress parameter
W_s	settling velocity ($m\,s^{-1}$)
W_{sFloc}	settling velocity corrected for flocculation and hindered settling ($m\,s^{-1}$)
z	depth below sediment surface for cohesive bed (m)
z_0	bed roughness (m)
η	dynamic viscosity (Pa s)
ν	kinematic viscosity ($m^2\,s^{-1}$)
ρ	fluid density ($kg\,m^{-3}$)
ρ_{clay}	density of the clay minerals ($kg\,m^{-3}$)
ρ_{dry}	dry bulk density of cohesive bed ($kg\,m^{-3}$)
ρ_s	density of non-cohesive sediment ($kg\,m^{-3}$)
ρ_{wet}	wet bulk density of sediment ($kg\,m^{-3}$)
τ_0	bed shear stress (Pa)
τ_{cd}	critical deposition shear stress for cohesive sediment (Pa)
τ_{ce}	critical erosion shear stress for cohesive sediment (Pa)
τ_{crb}	critical shear stress for initiation of bedload motion (Pa)
τ_{cs}	instantaneous skin-friction current shear stress (Pa)
τ_{cws}	the instantaneous skin-friction combined shear stress (Pa)
τ_{mUlva}	threshold of motion of vegetation (Pa)
$\tau_{resUlva}$	threshold of full resuspension of vegetation (Pa)
τ_{solid}	solid-transmitted stress (Pa)

Sediment-transport modelling started with the development of analytical and 1-D models (De Vries et al., 1989; Dyer and Evans, 1989; Grant and Madsen, 1979; Ross and Mehta, 1989; Smith, 1977; Wiberg et al., 1994). Due to recent advances in hydrodynamic and wave modelling as well as the increase in computing power, depth-averaged two-dimensional models (Harris and Wiberg, 2001; Li et al., 1994; Mulder and Udink, 1991) and three-dimensional models (Le Normant, 2000; Lesser et al., 2004; Pandoe and Edge, 2004) have evolved. The sophistication of model structure appears to have outstripped the understanding of sedimentary processes such as flocculation, consolidation, sand–mud interactions, and the theories on which they are based.

This paper describes the implementation of Sedtrans05, a one-dimensional (vertical) numerical model, which accounts more accurately than hitherto the complex sedimentary processes of coastal environments, giving not only boundary layer parameters but also predicting bedform development, bedload as well as suspended load transport rates for both sand and cohesive sediments. Our ability to realistically simulate sediment transport is often limited by our ability to formulate

essential sediment processes, not by the efficiency and sophistication of our numerical models. Sedtrans05 has been developed as a 1D model to test the model behaviour, to compare various algorithms between each other, and to calibrate them with field data. The simplicity and flexibility of 1D models also facilitate the incorporation of new processes, especially for cohesive sediments. On the other hand, multi-dimension models are needed to address spatial variability and seabed deposition/erosion pattern. However, once a 1D model has been tested it can be easily integrated into other 2D/3D models; see Ferrarin et al. (2004) for an example of integration of Sedtrans05 in a 3D hydrodynamic model.

Sedtrans05 is the latest version of SEDTRANS, which was developed more than 20 years ago (Davidson and Amos, 1985; Martec Ltd., 1987; unpublished reports by Martec Ltd.[2]). The two latest versions were SEDTRANS92 (Li and Amos, 1995) and SEDTRANS96 (Li and Amos, 2001). Sedtrans05 differs from SEDTRANS96 in several fundamental ways. The Fortran77 code is restructured so that all computations of the hydrodynamics and resulting sediment transport are accessed through a single subroutine that can be called from various programs. A new cohesive sediment algorithm is developed: (1) it provides detailed variations of sediment properties with depth, (2) it represents the suspended sediment as a spectrum of settling velocities (i.e. size classes), (3) it includes the flocculation process, and (4) it provides simulations of multiple erosion–deposition cycles. The Van Rijn (1993) method has been added to the equations available for prediction of non-cohesive sediment transport. Still water settling velocity of sand is computed with the equation of Soulsby (1997). Also, the density and viscosity of water are computed from temperature and salinity input data.

2. Model structure and program operation

Sedtrans05 is a one-dimensional (vertical profiles) model of sediment transport that simulates either sand or cohesive sediments under either steady currents or under the combined influences of waves and currents. Sedtrans05 uses the Grant and Madsen (1986) continental shelf bottom boundary layer theory to predict the mean bed shear stresses and the combined velocity profile.

Five methods to predict sediment transport for non-cohesive sediments are programmed into the newer version. The methods of Einstein–Brown (Brown, 1950), Yalin (1963), and Van Rijn (1993) predict bedload transport. The methods of Engelund and Hansen (1967) and Bagnold (1963) predict total load transport (bedload plus suspended load). The dimensions and type of bedforms are also predicted. A new algorithm for cohesive sediments determines more accurately bed erosion and deposition (see Section 4).

Sedtrans05 is composed of several linked elements. The calculations are coded in a set of Fortran77 routines that are accessed through the subroutine SEDTRANS05. This subroutine takes as input current and wave conditions and sediment type (Table 1). After calling the appropriate subroutines, the model returns the results as output.

The core subroutine SEDTRANS05 can be called in several ways: (1) as an interactive input and batch program—SED05—which runs in a console window; (2) as a graphic user interface—Sedtrans05 GUI—written in Visual Basic and running under Microsoft Windows; (3) as a MEX-file function to call the Fortran77 subroutines directly from Matlab—sedtrans05m; (4) as a 1D (time series) model for cohesive sediment—SEDI1D—which was used to calibrate the cohesive sediment algorithm (see Section 5.2); and (5) as a subroutine linked to a 3D hydrodynamic model, such as the model SHYFEM, which simulates waves and tidal flows in Venice lagoon (Ferrarin et al., 2004; Umgiesser et al., 2006).

Sedtrans05 can be used as 1D model or integrated into a multi-dimensional model. The difference is simply that in the 1D interface the velocities and wave parameters are prescribed as external forcing, supplied by the user, whereas in a 2D/3D model these values are supplied directly by the hydrodynamic model. Likewise, the output of Sedtrans05 is simply written to output files for a 1D interface, whereas, when integrated in a multi-dimensional model, the output is fed back to the hydrodynamic model to change the bathymetry; it therefore provides feedback from the sediment dynamics to the hydrodynamics.

[2]Martec Ltd., 1984. SED1D: a sediment transport model for the continental shelf. Unpublished report submitted to Geological Survey of Canada, DSS Contract no. 10SC 23420-3-M753, 63pp. Martec Ltd., 1990. Upgrading and application of the AGC sediment transport model SEDTRANS. Unpublished report submitted to Geological Survey of Canada, SCC Contract no. 23420-0-M166/01-OSC, 56pp.

Table 1
Input parameters for program SED05 and main subroutine SEDTRANS05

Variable	SED05 input	SEDTRANS05 input	Description
IRUN	X	X	Identifier for the run (integer value)
IOPT1	X	X	Selection of sediment transport Eqs. (1)–(5) or (7)
D	X	X	Water depth (m)
UZ	X	X	Current speed ($m\,s^{-1}$)
Z	X	X	Height of current measurement (m)
CDIR	X	X	Current direction (degrees north)
HT	X	X	Wave height (m)
PER	X	X	Wave period (s)
WDIR	X	X	Wave direction (degrees north)
GD	X	X	Grain size (m)
RHINP	X	X	Ripple height (m)
RLINP	X	X	Ripple length (m)
BETA	X	X	Bed slope (deg)
RHOS	X	X	Grain density
SALIN	X[a]		Salinity
TEMP	X[a]		Temperature (°C)
RHOW	[a]	X	Water density ($kg\,m^{-3}$)
VISC	[a]	X	Dynamic viscosity of water (Pa s)
TIMEDR	X[b]	X[b]	Duration of deposition/erosion (s)
AULVA	X[b]	X[b]	Fraction of bed area covered by free moving vegetation
CONC	X[b]	X[b]	$C_{(i)}$ for each W_s class (array)
NBED	X[b]	X[b]	Number (N) of entries in BEDCHA
z1–zN	X[b]		Depth (positive downward, m)
rho1–rhoN	X[b]		Dry bulk density ($kg\,m^{-3}$)
tero1–TeroN	X[b]		Critical erosion stress (Pa)
BEDCHA		X[b]	Bed characteristics (array)

[a]RHOW and VISC can be entered into SED05 instead of SALIN and TEMP with the special command-line argument "−v".
[b]Used only for the cohesive sediment algorithm.

Sedtrans05 is licensed under the GNU General Public Licence. The Fortran77 source code is available from the web site of *Computers & Geosciences*. In addition, executables of SED05 and SEDI1D compiled for DOS/Windows and for Linux, and the graphic user interface for Windows (Sedtrans05 GUI) are available at http://labsedim.uqar.qc.ca/sedtrans05.

2.1. Program operation

A user manual, which explains in detail the program operation, is distributed with the program. Therefore, only the main characteristics of the different components are summarized here.

SED05 is a user interface that runs in a console window. It computes sediment transport for a given set of conditions. The command-line option "−?" displays the explanations of the command-line syntax (Appendix A). By default, SED05 starts in interactive mode, asking for the input values to be introduced by the user at the command line. Alternatively, with a command-line option, the program reads input values from a prepared input data file and computes results in batch mode. The results are written in five output files of the same name but different extensions: that is, a text file with the input values and the summary of the results; and four tabular ASCII files with all the output parameters. The command-line option "−e" generates an example input file and an explanation file for the output files.

Sedtrans05 GUI operates in the same way as SED05 for the non-cohesive methods, with the added advantage of showing all the input and output parameters simultaneously in the application window.

Sedtrans05m operates in the same way as SED05. It has the advantage that, if the input data are already in Matlab and the output is afterward processed in Matlab, it is not necessary to generate an input data file and then to read the output data files.

SEDI1D is an interface to Sedtrans05 that simulates a 1D (vertical)-time model for cohesive sediments. It assumes an infinite, homogeneous, horizontal bed, which is subject to time-varying current and wave conditions. This simple model is adapted for the simulation of processes observed in flumes. The input parameters are the initial bed characteristics, the initial suspended sediment concentration (SSC), and several successive hydrodynamic conditions, each with a specific duration. The output is a tabular file with SSC and bed characteristics.

Several equations, which are used by the cohesive sediment algorithm, contain coefficients that are not constant, but may vary depending on sediment type or further advances in our understanding. The user is able to modify these coefficients to their needs without modification to the source code. All these coefficients (Table 2) are stored in a common block—CCONST, which is initialized with default values by calling the subroutine INICONST before the first computation. Some or all coefficients can then be customized with a call to the subroutine SETCCONST, which reads the new values in a customization file. This file is specified as a command-line argument for SED05 and SEDI1D.

2.2. Limitations of Sedtrans05

Sedtrans05 is written in Fortran77 and was developed with the compiler g77. The program uses a few extensions to the Fortran77 standard, which are supported by most compilers (see the user manual). The SED05 input interface also uses two compiler-specific functions to retrieve command-line arguments, but the code can be easily modified to skip this action.

The core subroutine SEDTRANS05 does not undertake argument checks. Thus failure of the user to give realistic input arguments may cause the program to crash. There is a limited argument check in the user interfaces SED05 and Sedtrans05 GUI. Sedtrans05 assumes linear wave theory, i.e. it does not model breaking waves. It is the responsibility of the user to assure that the input conditions are within the range of validity of the different equations used.

Sedtrans05 assumes linear eddy viscosity and neglects the effect of suspended sediment stratification in the suspended load transport calculation. Therefore caution should be applied when the model is used for deep water or stratified conditions.

Table 2
Coefficients for cohesive sediment equations, which are stored in common block CCONST

Variable	Default value	Description
CSULVA	159.4	C_{solid} coefficient for the solid-transmitted stress by free-moving vegetation
TMULVA	1.054e−3	τ_{mUlva} threshold of motion of vegetation (Pa)
TRULVA	0.0013	$\tau_{resUlva}$ threshold of full resuspension of vegetation (Pa)
RKERO	1.95e−5	P_e, erosion proportionality coefficient
E0	5.88	E_0, minimum erosion rate
CDISRUPT	0.001	D_t, constant for turbulent floc disruption
CLIM1	0.1	C_{LIM1}, limit for flocculation equations ($kg\,m^{-3}$)
CLIM2	2.0	C_{LIM2}, limit for flocculation equations ($kg\,m^{-3}$)
KFLOC	0.001	F_k, flocculation constant
MFLOC	1	F_m, flocculation constant
RHOCLAY	2600	ρ_{clay}, density of clay minerals ($kg\,m^{-3}$)
CTAUDEPK	2800	k_{cd}, coefficient for computing τ_{cd}
CTAUDEPM	1.03	m_{cd}, coefficient for computing τ_{cd}
PRS	0	P_s, resuspension probability (range 0–1)
RHOMUD	50	Density of the freshly deposited mud ($kg\,m^{-3}$)
DPROFA	470	Constant D_a for final density profile
DPROFB	150	Constant D_b for final density profile
DPROFC	0.015	Constant D_c for final density profile
DPROFD	0	Constant D_d for final density profile
DPROFE	0	Constant D_e for final density profile
CONSOA	1e−5	C_a time constant of consolidation
TEROA	6e−10	T_a constants for erosion threshold from density and overlaying mass
TEROB	3	T_b
TEROC	3.47	T_c
TEROD	−1.915	T_d
CDRAGRED	−0.0893	C_{dr} constant for the drag reduction formula ($m^3\,kg^{-1}$)
WSCLAY	5	Primary median W_s class (integer value)
ZOCOH	2e−4	z_0 bed roughness for cohesive sediments (m)
FCWCOH	2.2e−3	Friction factor for cohesive sediments
DOCOMPACT	0	If not zero, call COMPACT within COHESIVE

They can be modified by the user.

The *cohesive sediment algorithm* does not model sand–mud mixtures, lateral movement of fluid mud (due to current or gravitational forces), resuspension of fluid mud by waves, instabilities of the water–sediment interface (Helmholtz waves), and the influence of currents on sediment consolidation. The flocculation equations are valid for seawater and brackish water with a salinity down to about 10–15 psu. Therefore it should not be used for fresh water or very low salinities. Biological processes (bioconsolidation or bioturbation) are not mod-

elled, but the program structure allows for the addition of a biological module modifying the bed characteristics outside the core part of Sedtrans05. The cohesive sediment algorithm may not predict correctly erosion rate when long (much longer than 5 min) time steps (TIMEDR) are used.

3. Hydrodynamic and non-cohesive subroutines

3.1. Hydrodynamic calculations

The hydrodynamic calculations (boundary layer parameters, threshold for sediment transport, etc.) have been modified from SEDTRANS96 as described below. The reader is referred to Li and Amos (2001) for detailed theories of the program.

3.1.1. Density and viscosity of water

Water density (ρ) and dynamic viscosity (η) are computed from temperature and salinity in the user interface (subroutine DENSVISC) and are then transmitted to the core subroutine SEDTRANS05. This avoids redundant computation when SEDTRANS05 is called from 3D models where ρ and η may be known. The water density is computed according to the equation of state for seawater EOS80 (Fofonoff, 1985). An expression of dynamic viscosity as a function of temperature (T, in °C) and salinity (S) is determined from data presented by Riley and Skirrow (1965, Table 25):

$$\eta = 1.802863 \times 10^{-3} - 6.1086 \times 10^{-5} T + 1.31419 \times 10^{-6} T^2 - 1.35576 \times 10^{-8} T^3 + 2.15123 \times 10^{-6} S + 3.59406 \times 10^{-11} S^2 \quad (1)$$

The error of this formula compared to the data of Riley and Skirrow (1965) is less than 0.5% over the salinity range 0–38 and the temperature range 8–24 °C. The error is less than 1.0% over the temperature range 0–28 °C.

3.1.2. Settling velocity

Sedtrans96 used the formula of Gibbs et al. (1971), which computes the settling velocity (W_s) of spherical grains. Sedtrans05 uses the more recent formula of Soulsby (1997), which is more adapted to natural sand grains:

$$W_s = \frac{v}{D}[(10.36^2 + 1.049 D_*^3)^{0.5} - 10.36] \quad (2)$$

where v is the kinematic viscosity (η/ρ), D is the median sieve grain diameter, and D_* is the dimensionless grain size computed as

$$D_* = \left[\frac{g(\rho_s/\rho - 1)}{v^2}\right]^{1/3} D \quad (3)$$

where g is the acceleration due to gravity and ρ_s is the grain density.

3.1.3. Critical shear velocity for initiation of resuspension

The critical shear velocity for sediment suspension (u_{*crs}) is computed following the Van Rijn method (Van Rijn, 1993):

$$1 < D_* \leqslant 10 : \frac{u_{*crs}}{W_s} = \frac{4}{D_*}$$
$$D_* > 10 : \frac{u_{*crs}}{W_s} = 0.4 \quad (4)$$

The criterion of Bagnold (1966; adopted in Sedtrans96) may define the upper limit at which a concentration profile starts to develop, while the Van Rijn method defines an intermediate stage at which locally turbulent bursts lift sediment particles from the bed into suspension (Van Rijn, 1993).

3.1.4. Friction factor and z_0 for cohesive sediments

Sedtrans05 computes the friction factor and the bed roughness (z_0) for non-cohesive sediment from the grain size and the predicted bedforms. For cohesive sediment, a default friction factor (0.0022) and a default z_0 (0.0002 m) are defined using values proposed by Soulsby (1983). The default values are stored in the common block CCONST and may be modified by the user. Sedtrans05 does not predict bedforms for cohesive sediments. If height and length of ripples are given as input, the values are not used in the computation, but are simply copied to the output of predicted bedform dimensions.

3.2. Transport equations

Four methods were used in SEDTRANS96 to predict the sediment transport for non-cohesive sediments: the methods of Einstein–Brown (Brown, 1950) and Yalin (1963) estimate the bedload transport, and the methods of Engelund and Hansen (1967) and Bagnold (1963) estimate the total load transport (bedload plus suspended load). These methods are described in Li and Amos (2001). In Sedtrans05 the Van Rijn (1993) bedload algorithm has been included to estimate more accurately sediment-transport rate of fine sand. The suggested applicable grain-size range for each method is

reported in Table 3. However, the method should not be principally selected according to the grain size, but the other assumptions of each method must also be considered.

3.2.1. Van Rijn bedload equation

Van Rijn (1993) followed the approach of Bagnold assuming that the motion of the bedload particles is dominated by saltation under the influence of hydrodynamic fluid forces and gravity. The saltation characteristics have been determined by solving the equations of motion for an individual particle. The bedload transport rate is defined as the product of the particle velocity, the saltation height, and the bedload concentration. It is assumed that the instantaneous bedload transport rate is related to the dimensionless shear stress parameter (T_m).

The bedload transport rate (q) for the pure current case is

$$q = \alpha(s-1)^{0.5} g^{0.5} D^{1.5} D_*^{-0.3} T_m^{2.1} \quad (5)$$

where s is the ratio of density of sediment and water, α is a constant equal to 0.053, and T_m is computed as

$$T_m = \frac{\tau_{cs} - \tau_{crb}}{\tau_{crb}} \quad (6)$$

where τ_{cs} is the instantaneous skin-friction current shear stress and τ_{crb} is the critical shear stress for initiation of bedload motion.

The instantaneous bedload transport rate for the combined current and wave case is

$$q = 0.25\alpha D D_*^{-0.3} \left(\frac{\tau_{cws}}{\rho}\right)^{0.5} T_m^{1.5} \quad (7)$$

where $\alpha = 1\text{–}(H_s/h)^{0.5}$ is a calibration factor, H_s is the significant wave height (m), h is the water depth (m), τ_{cws} is the instantaneous skin-friction combined shear stress, and T_m for the combined-flow case is defined as

$$T_m = \frac{\tau_{cws} - \tau_{crb}}{\tau_{crb}} \quad (8)$$

The time-averaged bedload transport rate is obtained by averaging over a wave period.

Table 3
Summary of different transport equations for non-cohesive sediment

Method	Transport mode	Grain-size (mm)
Engelund–Hansen (1967)	Total load	>0.15[a]
Einstein–Brown (1950)	Bedload	0.3–28.6[b]
Bagnold (1963)	Total load	0.18–0.45[b]
Yalin (1963)	Bedload	>0.2[a]
Van Rijn (1993)	Bedload	0.05–29.1[a]

[a]Grain-size range recommended for using the method according to the literature.

[b]Grain size of experiments, which the method is based on.

4. The cohesive sediment algorithm

The cohesive sediment subroutine of Sedtrans05 has been rewritten. It uses the same basic erosion and deposition equations as SEDTRANS96. The cohesive sediment algorithm is designed to model a full cycle of erosion–deposition as well as bed consolidation. This is achieved by two array variables, which contain detailed characteristics of the bed and the SSC. These array variables are input arguments that are modified by Sedtrans05, and are then returned as output arguments. Sediment mass is conserved throughout the periods of erosion, deposition, and consolidation. In addition, several processes that were not modelled in SEDTRANS96 are now included. These are: (1) the inclusion of multiple classes of suspended sediment with differing W_s; (2) the estimation of W_s of aggregates eroded from the bed computed based upon the stress history that lead to the erosion of these aggregates; (3) the mechanism of flocculation; and (4) bed consolidation. For some of these processes, there is no well-accepted formula, and for some experimental data are sparse.

4.1. Program flow

Erosion and deposition may occur simultaneously in Sedtrans05, depending on the erosion threshold of the bed surface and the settling-velocity distribution of the concomitant suspended sediment. However, freshly eroded sediment does not deposit under the same flow conditions; similarly freshly deposited sediment does not erode in the same flow conditions. Therefore, simultaneous erosion and deposition will only occur in rare cases with rapid change in flow conditions.

The cohesive sediment algorithm is contained in the subroutine COHESIVE and several subroutines that are called from there. Each call to the subroutine COHESIVE has a specific time step, Δt. For general modelling, a time step of 300 s (5 min) is considered optimum. Results may not be accurate with longer time steps, especially in the presence of significant flocculation or a strong

gradient of critical erosion shear stress (τ_{ce}) with depth. A time step of 20 s was used in the calibration to reproduce processes in a field flume with accurate measurements of flow and SSC. For each time step, the calculations are performed in the following order:

(1) the computation of the effective bed shear stress τ_0 taking into account drag reduction due to high SSC and drag enhancement due to solid-transmitted stress;
(2) the mass of eroded sediment and erosion of the bed is computed (first part of erosion calculation);
(3) deposition (which includes flocculation), deposition rate for each W_s class, removal of the deposited mass from the suspended sediment load, and addition of the freshly deposited sediment to the bed are calculated;
(4) the mass of eroded sediment is added to the suspended sediment load (second part of erosion calculation); and
(5) consolidation of the bed is evaluated (optionally).

The cohesive sediment algorithm takes as input the following arguments: bed characteristics, the W_s distribution, τ_0, the fraction of the bed covered by debris involved in the solid-transmitted stress, and Δt. The following output is returned at each time step: final bed characteristics, the final W_s distribution, the final SSC, the mean erosion–deposition rate, the change in bed height, the solid-transmitted stress (τ_{solid}), and the effective stress including corrections for drag reduction and τ_{solid}.

4.2. Representation of the sediment bed

Sedtrans05 uses dry bulk density (ρ_{dry}) to describe the bed (this has units of sediment mass concentration), because it simplifies the mass-conservation calculation. The often-measured wet bulk density ρ_{wet} can be converted to ρ_{dry} with the formula

$$\rho_{dry} = (\rho_{wet} - \rho)\frac{\rho_{clay}}{\rho_{clay} - \rho} \quad (9)$$

where ρ_{clay} is the mineral density of the sediment. The variation of bed characteristics with depth is represented by two profiles of τ_{ce} and ρ_{dry}. The information is stored in a three-column table (a two-dimensional array), containing depth, τ_{ce}, and ρ_{dry}. This corresponds to a bed composed of several layers, each with linear variations of τ_{ce} and ρ_{dry}. Each row in the table specifies a limit between layers; the first row is always the surface. The bed characteristics are assumed to be constant below the depth specified in the last row of the table (Fig. 1). The number of layers is variable between 0 (depth invariable bed) and 49, depending on initial user input and subsequent erosion–deposition history.

If a layer is completely eroded, it is removed from the table and the remaining layers are moved upward. If a layer is only partially eroded, the surface values of τ_{ce} and ρ_{dry} are updated assuming a linear variation in the uppermost layer. If deposition to the bed is predicted, a new layer is inserted to the top of the table; however, if the characteristics of the uppermost layer are close to freshly deposited sediment, the uppermost layer will simply be increased in thickness (Fig. 1C).

The reference depth is always the sediment surface. After each phase of erosion or deposition, all depth values are corrected accordingly. The effective variation of surface elevation during each time step is an output of Sedtrans05.

4.3. Representation of suspended sediments

The suspended sediment population is divided in several classes to represent the natural size distribution of suspended sediment, each characterized by its settling velocity $W_{s(i)}$ and concentration $C_{(i)}$. The number of classes must be specified before compiling. In this version, 21 classes are used that are equally log-spaced from 0.00001 to 0.1 m s^{-1} (the ratio of W_s between two successive classes is 1.58). The number of classes may be adjusted from 5 to 30. Using a small number of classes may be appropriate for coupling Sedtrans05 with larger 3D models. The median W_s of each class is computed by the subroutine INICCONST and is stored in the common block WSCLASS. It is also written to one of the output files.

Each suspended particle is assumed to have a characteristic W_s, which is defined during the erosion process when the particle is put into suspension (see below, under "erosion"); this value it retains until the particle is deposited. However, it may be modified temporarily to take into account flocculation (see below).

Particles with a log-normal distribution of W_s are put into suspension at each erosion step (Fig. 2A). The median of this distribution depends on the erosion conditions (see below). Successive erosion

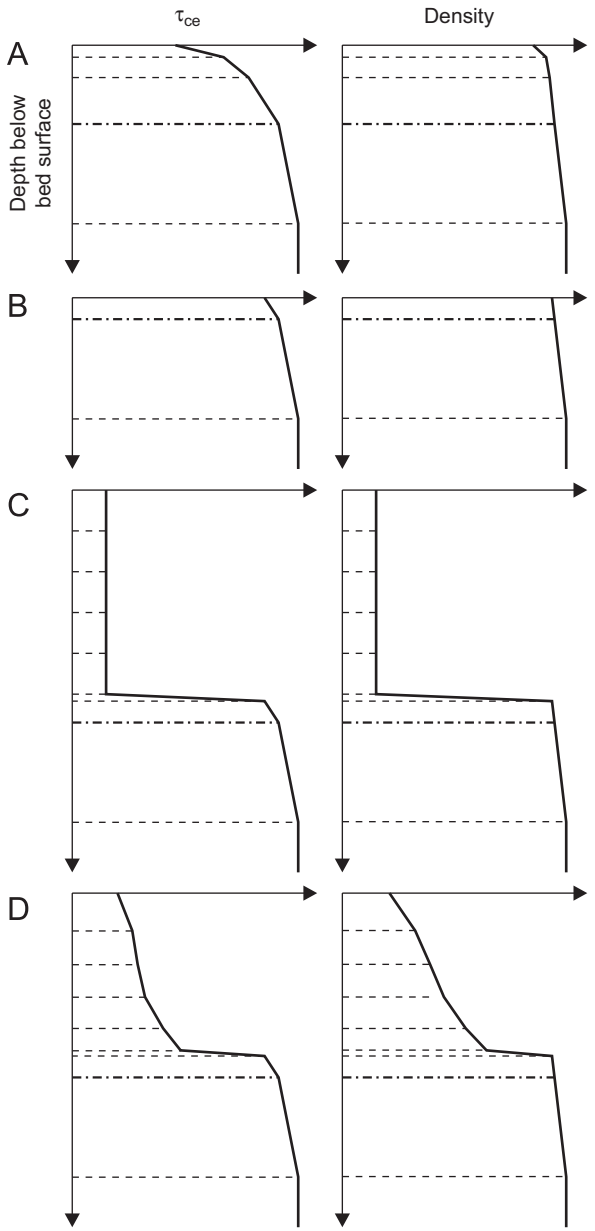

Fig. 1. Examples of cohesive-bed characteristics (critical shear stress of erosion τ_{ce} and density ρ_{dry}) at four instants of an erosion–deposition–consolidation cycle. Dashed lines mark limits between layers. Lowest layer has a constant τ_{ce} and ρ_{dry}. (A) Natural consolidated bed (five layers). (B) Same bed truncated by erosion (three layers). (C) Same bed just after deposition of fresh sediment (nine layers). (D) Same bed after consolidation (nine layers).

steps under different conditions generate a complex W_s distribution (Fig. 2B). The deposition rate of each W_s class is computed separately from the erosion process, the coarsest particles being deposited fastest (Fig. 2C). This represents well the phenomenon called the degree of retention, i.e., the fraction of sediment remaining indefinitely in suspension within a given steady current.

4.4. Bed shear stress

Bed shear stress τ_0 is corrected for two phenomena that might take place in flows moving over cohesive (fine-grained) beds: drag reduction due to high SSC and the presence of a solid-transmitted stress (τ_{solid}) by moving detritus of low density. Firstly, τ_0 (the skin-friction stress computed in the hydrodynamic routine) is corrected for drag reduction. Then, τ_{solid} is calculated from this corrected τ_0 and is added to it.

A water–sediment mixture does not behave as a Newtonian fluid at high values of SSC. Therefore, the effective τ_0 felt by the bed (and which creates erosion) is lower for given current speed due the phenomenon of drag reduction (Best and Leeder, 1993). Neumeier et al. (in prep.) defined a correction factor to the computed τ_0 by fitting an exponential

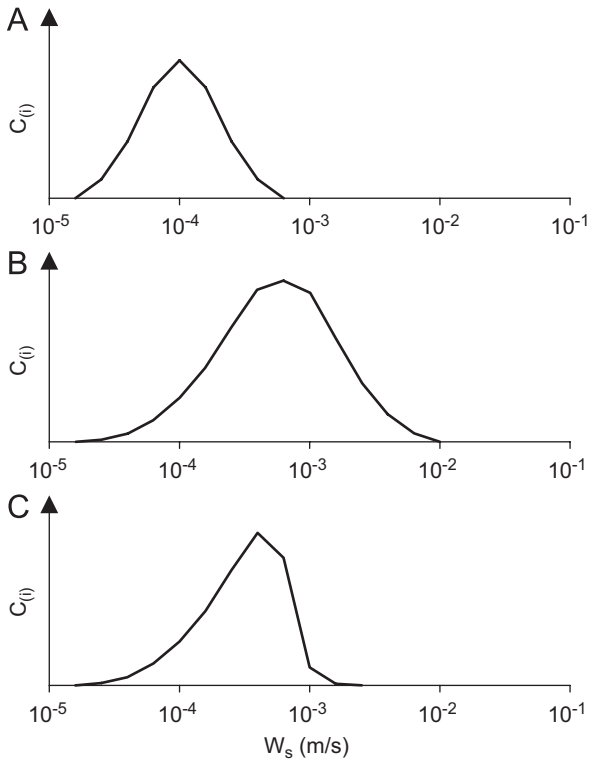

Fig. 2. Examples of W_s distribution for sediment in suspension. (A) Log-normal distribution that is put into suspension. (B) W_s distribution after a complex erosion history. (C) W_s distribution after settling of coarsest particles.

best-fit to the data of Li and Gust (2000):

$$\tau_{0\,\mathrm{corrected}} = \exp(C_{\mathrm{dr}}\mathrm{SSC})\,\tau_{0\,\mathrm{uncorrected}} \quad (10)$$

where C_{dr} is a constant ($-0.0893\,\mathrm{m^3\,kg^{-1}}$). With this formula, τ_0 is halved for each increase in concentration by $7.8\,\mathrm{kg\,m^{-3}}$. The experimental data on drag reduction result from flume experiments with unidirectional currents. Therefore, this correction may not be adapted for combined current-wave flows, and SSC in Eq. (10) corresponds to the concentration less than 0.5 m from the boundary.

The use of Sedtrans05 in Venice lagoon (Umgiesser et al., 2006) was one of the motivations for the upgrade of Sedtrans96. A significant amount of the lagoon bed is covered periodically by a freely moving green alga (*Ulva rigida*) that is known to apply a solid-transmitted stress τ_{solid} to the bed when the alga is in motion (Flindt et al., 2004). Laboratory experiments in a large annular flume (Cozette, 2000) have shown that (1) *Ulva* has a distinct threshold of motion τ_{mUlva}; (2) τ_{solid} is proportional to the bed fraction covered by *Ulva* (A_{ulva}) and to the excess stress above τ_{mUlva}; and (3) *Ulva* is fully suspended (without generation of τ_{solid}) above a second threshold τ_{resUlva}. A linear decrease of τ_{solid} is assumed above 0.8 τ_{resUlva}, to represent the transition from bedload to suspension:

$$\tau_{\mathrm{solid}} = A_{\mathrm{ulva}} C_{\mathrm{solid}}(\tau_0 - \tau_{\mathrm{mUlva}}) \quad \text{for } \tau_{\mathrm{mUlva}} < \tau_0 < 0.8\tau_{\mathrm{resUlva}} \quad (11)$$

$$\tau_{\mathrm{solid}} = A_{\mathrm{ulva}} C_{\mathrm{solid}}(0.8\tau_{\mathrm{res}} - \tau_{\mathrm{mUlva}}) \frac{\tau_{\mathrm{resUlva}} - \tau_0}{0.2\tau_{\mathrm{resUlva}}} \quad \text{for } 0.8\tau_{\mathrm{resUlva}} < \tau_0 < \tau_{\mathrm{resUlva}} \quad (11a)$$

where C_{solid} is an experimentally determined coefficient (159.4), $\tau_{\mathrm{mUlva}} = 0.001054\,\mathrm{Pa}$, and $\tau_{\mathrm{resUlva}} = 0.0013\,\mathrm{Pa}$. C_{solid}, τ_{mUlva}, and τ_{resUlva} are stored in the common block CCONST (Table 2) and can be modified to model τ_{solid} produced by other objects based upon the same principles as those applied to *Ulva*.

4.5. Bed erosion

If τ_0 is higher than the critical shear stress for erosion of the bed surface $\tau_{\mathrm{ce}(0)}$, then sediment erosion will occur. The mass erosion rate r_{e} is defined using a standard formula for beds with variable τ_{ce} (Amos et al., 1992; Parchure and Mehta, 1985; Van Rijn, 1993):

$$r_{\mathrm{e}} = \partial m/\partial t = E_0 \exp[P_{\mathrm{e}}(\tau_0 - \tau_{\mathrm{ce}(z)})^{0.5}] \quad (12)$$

where E_0 is an empirical coefficient for minimum erosion, P_{e} is the proportionality coefficient for erosion, and $\tau_{\mathrm{ce}(z)}$ is the critical shear stress for erosion as a function of erosion depth.

For each time step, r_{e} is first computed with the surface τ_{ce}, then the eroded depth Δz is computed (taking into account the linear variation of ρ_{dry} with depth). If Δz is deeper than the first bed layer, then the time to erode the first layer is calculated and the operations are repeated on the next layer with the remaining time. If $\tau_{\mathrm{ce}(\Delta z)}$ is equal to or lower than τ_0, then the erosion is stopped at the first depth where $\tau_{\mathrm{ce}(z)} = \tau_0$.

The calibration with SEDI1D revealed that the coefficients E_0 and P_{e} (Eq. (12)) are not universal, but depend on local conditions (Table 4). In addition, τ_0 may vary up to one order of magnitude depending on which method is used to measure and compute it (Thompson et al., 2003); this directly influences P_{e}. Therefore it may be necessary to adjust the coefficients in the erosion equation during the calibration process.

4.5.1. Settling velocities of eroded sediment

A log-normal distribution of seven W_{s} classes is put in suspension at each erosion step (Fig. 2A). The median of this distribution depends on the erosion conditions (see below). The standard deviation of this distribution, computed using $\log_{10}(W_{\mathrm{s}})$, is 0.3.

By default, a *primary* W_{s} distribution is put into suspension, which corresponds to the finest possible suspension for a given bed sediment composition. This distribution is defined with the parameter WSCLAY (Table 2), the index of the median W_{s} class (default value 5, i.e. $W_{\mathrm{sn\ primary}}$ of $6.3\mathrm{e}{-5}\,\mathrm{m\,s^{-1}}$). The W_{s} distribution is shifted to higher values according to (1) the lifting capacity of the current (Bagnold, 1973; Dyer, 1986); (2) the size

Table 4
Different values for coefficients of the cohesive-sediment erosion equation (Eq. (12))

	P_{e}	E_0
Amos et al. (1992)[a]	1.62	51×10^{-6}
Sea Carousel Venice 99[b]	5.88	19.5×10^{-6}
Miniflume Venice 99[b]	4.68	6.7×10^{-6}

Mehta (1988) summarizes in his Table 3 other experimental values for these coefficients.

[a]Used in SEDTRANS96.

[b]Computed from data of Amos et al. (2000).

of the eroded aggregates, which increases with increasing consolidation (Droppo et al., 2001; Perkins et al., 2004); and (3) the turbulent breakdown of suspended aggregates (Kranck and Milligan, 1992). The maximum W_s class that can be suspended (rule 1) is defined as W_{lift}:

$$W_{lift} = (\tau_0/(0.64\rho_{water}))^{0.5} \quad (13)$$

The maximum W_s class that is strong enough to resist disruption by the turbulence (rules 2 and 3) is defined as $W_{disruption}$:

$$W_{disruption} = D_t \tau_{ce}/\tau_0^{0.5} \quad (14)$$

where D_t is a coefficient (Table 2, default value 0.004). The maximum W_s of particles put in suspension W_{sn} (coarse end of the W_s distribution) is then computed as the smaller of W_{lift} and $W_{disruption}$; however, if the result is smaller than the coarse end of the primary W_s distribution, the latter value is taken. This method does not take into account biological activity that may significantly increase W_s of eroded flocs due to bioconsolidation or pelletization of the sediment (Andersen and Pejrup, 2002; Perkins et al., 2004).

4.6. Flocculation–deposition

4.6.1. Flocculation

The set of equations of Whitehouse et al. (2000) is used for the computation of flocculation-hindered settling velocity W_{sFloc} as a function of suspended sediment concentration C. Firstly, the effective floc density ρ_{floc}, the volume concentration of flocs in water C_f, the length scale L, the effective diameter d_e, and the dimensionless floc diameter D_* are computed, and then the median settling velocity W_{sFloc} is computed as follows:

$$\rho_{floc} = \rho + C_{in}(\rho_{clay} - \rho) \quad (15)$$

$$C_f = \frac{(\rho_{clay} - \rho)C}{(\rho_{floc} - \rho)} \quad (16)$$

$$d_e = LC^{Fm/2}$$

$$L = \left[\frac{19.8\rho\nu\rho_{clay}^{Fm}F_k}{g(\rho_{floc} - \rho)}\right]^{1/2} \quad (17)$$

$$D^* = d_e\left[\frac{g(\rho_{floc} - \rho)}{\rho\nu^2}\right]^{1/3} \quad (18)$$

$$W_{sFloc} = \nu/d_e[(10.36^2 + 1.049(1 - C_f)^{4.7}D_*^3)^{0.5} - 10.36] \quad (19)$$

where C_{in} is the internal volume concentration of flocs (0.025–0.04, default value 0.03), F_k and F_m are two flocculation coefficients with default values 0.001 and 1 (Whitehouse et al., 2000). F_k and F_m are dependent on the sediment characteristics and seem to be different from one estuary to another; the user can modify them.

To save computation time, no flocculation is calculated below the concentration limit C_{LIM1} (default value 0.1 kg m^{-3}), and a simple equation is used between C_{LIM1} and C_{LIM2} (default value 2 kg m^{-3}): $W_{sFloc} = F_k C^{F_m}$ (Van Rijn, 1993). For concentrations between C_{LIM2} and 50 kg m^{-3}, the equations of Whitehouse et al. (2000) are used (Eqs. (15)–(19)). These equations are undefined at high concentrations. Thus the equation $W_{sFloc} = 0.00462\ (1 - 0.01\ C)^{3.54}$ is used for concentrations between 50 and 82 kg m^{-3} (Van Rijn, 1993), and a constant $W_{sFloc} = 10^{-5}$ m s^{-1} is assumed for concentrations above 82 kg m^{-3}.

Flocculated particles do not have a unique W_s but are still distributed over a certain range. This range is simulated by calculating for each original $W_{s(i)}$ a new $W_{s(i)Floc}$ such that

$$W_{s(i)Floc} = W_{sFloc}\sqrt{W_{s(i)}/W_{sMean}} \quad (20)$$

where W_{sMean} is the log-mean settling velocity of the original distribution. W_{sMean} is computed with

$$\log(W_{sMean}) = \frac{\sum C_{(i)}\ \log(W_{s(i)})}{SSC} \quad (21)$$

where $C_{(i)}$ is the concentration for each W_s class and SSC is the total concentration. This produces a distribution with a log-mean value equal to W_{sFloc}, and a shape similar to the shape of the original distribution. The standard deviation of this distribution, computed using $\log_{10}(W_s)$, is halved compared to the original distribution.

4.6.2. Deposition

Deposition occurs only when the bed shear stress τ_0 is less than the critical shear stress for deposition τ_{cd}, which is computed for each W_s class from $W_{s(i)Floc}$ using the relationship proposed by Mehta and Lott (1987):

$$\tau_{cd} = k_{cd} W_s^{m_{cd}} \quad (22)$$

where m_{cd} and k_{cd} are two coefficients. In settling experiments with an annular flume that will be

published elsewhere (Neumeier et al., in prep.), we found values between 0.9 and 1.4 for m_{cd}, and values between 1900 and 9000 for k_{cd}. The default values in Sedtrans05 are $m_{cd} = 1.03$ and $k_{cd} = 2800$; these coefficients can be modified by the user.

Sedtrans05 uses the same deposition equation as Sedtrans96, which was first defined in 1962 by Krone (1993). This equation exists in two forms: (1) as a deposition rate or (2) integrated over time to compute the concentration remaining in suspension C_t after a time interval t as a fraction of the initial concentration C_0:

$$r_d = \partial m/\partial t = CW_s(1 - \tau_0/\tau_{cd})(1 - P_s) \quad (23)$$

$$C_t = C_0 \exp\left(-W_s(1 - \tau_0/\tau_{cd})(1 - P_s)\frac{t}{h}\right) \quad (23a)$$

where P_s is a dimensionless probability coefficient of resuspension in the depositional state (ranging from 0 to 0.2 with a default value of 0). The deposition of each class of suspended sediment is computed separately. All sediment of a class is deposited when the concentration of that class falls below $0.0001\,kg\,m^{-3}$.

4.6.3. Characteristics of freshly deposited sediment

The freshly deposited sediment is assumed to be a fluid mud with a fixed density specified by RHOMUD (Table 2, default value $50\,kg\,m^{-3}$, Whitehouse et al., 2000). τ_{ce} is set through application of the following rules: (1) τ_{ce} is 10% higher than τ_0 to avoid immediate resuspension (see also Droppo et al., 2001); (2) τ_{ce} has a minimum value computed from ρ_{dry} with Eq. (25); and (3) τ_{ce} of a new layer must not be greater than the underlying bed surface.

4.7. Consolidation

Self-weight consolidation of recently deposited cohesive sediment is an important process that increases bed stability. Hence it should be included in sediment-transport models. Self-weight consolidation is controlled by sediment permeability that limits the escape of interstitial water (Sills, 1997). This depends on many parameters such as mineralogy, interstitial fluids, sand content, etc. (Migniot, 1989). Detailed models have been proposed (Pane and Schiffman, 1985; Sanchez and Grovel, 1994; Toorman, 1996; Winterwerp and van Kesteren, 2004), but they are too complex and computation intensive for a general sediment-transport model.

For this reason, we tried to develop a simplified, empirical numerical model based on the following principles: (1) the controlling parameter of consolidation is the buoyant weight of the overlaying sediment and the depth below the sediment surface; (2) a stable density profile (ρ_{final}) would be reached after an infinite time; and (3) $\tau_{ce}(z)$ depends on ρ_{dry} and the mass of overlaying sediments. The density increases according to the relationship

$$\rho_1 = f(\rho_0, m_o, z, \Delta t) \quad (24)$$

where ρ_0 is the initial density, ρ_1 the density after a time step Δt, m_o is the mass of overlaying sediment, and z is the depth. Due to uncertainties in defining and calibrating the empirical Eq. (24), it is deactivated as a default in Sedtrans05.

The *erosion threshold* τ_{ce} is generally linked to the density, typically with a formula such as $\tau_{ce} = a\rho_{dry}^{b}$ (Van Rijn, 1993; Whitehouse et al., 2000). However, this relationship is only valid for the bed surface. τ_{ce} increases rapidly with depth below the surface, while ρ_{dry} changes only slowly (Amos et al., 2000). Therefore we used a modified formula that includes also a contribution from m_o:

$$\tau_{ce} = T_a\rho_{dry}^{Tb}(1 + T_c(1 - \exp(T_d m_o))) \quad (25)$$

where T_a, T_b, T_c, and T_d are coefficients (default values 6e−10, 3, 3.47, −1.915) that were fitted using data presented in Amos et al. (2000, 2004). This equation with default coefficient characterizes well a standard bed, with the part in brackets modelling the typical curve of τ_{ce} increase with depth. However, natural cohesive sediments are highly variable (Black et al., 2002) and the coefficients must probably be adapted to local conditions. The previous value of τ_{ce} is not modified, if τ_{ce} computed from ρ_{dry} and m_o is lower than the previous value. The variations of both ρ_{dry} and τ_{ce} are computed for the limits between each sediment layer. It is assumed that both characteristics will vary linearly between these depths. Consolidation is computed if the parameter DOCOMPACT (Table 2) is different from 0.

5. Model calibration

5.1. Non-cohesive model validation

The non-cohesive sediment-transport algorithms have been compared against three experimental data sets. Two data sets were taken in the Sable Island Bank region, Scotian Shelf, and have been

previously used for the calibration of Sedtrans96 (Li and Amos, 2001). The first data set (SIB93) was collected by the GSCA instrumented tripod RALPH in 39 m water depth on medium sand sediment ($D = 0.34$ mm) in early winter of 1993. The second data set (SIB82) was collected with a similar tripod in 57 m water depth on fine sand (0.23 mm) in 1982. They correspond to mixed wave-current conditions on an open shelf. The detailed description of field methods, instrumentation, and data analyses are given in Li et al. (1997) and Li and Amos (1999).

The third data set (Venice) comes from a study on sand transport in Venice lagoon in autumn 2006 (Amos et al., 2007). Measurements of sand transport were made in Lido and Chioggia inlets in 4 and 8 m of water, respectively. Two Helley–Smith sand traps and a surface sampler (all equipped with 63 μm mesh sizes) were deployed synchronously from a boat for periods of 20 min duration and for a total of 12 profiles in each inlet. The region is strongly tidal and waves were absent. The trapped sediments correspond to well-to-moderately well sorted, very fine sand ($96 < D_{50} < 129$ μm). The water-velocity input for Sedtrans05 was derived from ADV flow measurements in Lido (Amos et al., 2007), while results from the SHYFEM hydrodynamic model (Umgiesser, 1997) have been used in Chioggia due to lack of field measurements.

The model predictions computed with the current, waves, and grain-size recorded in the field have been compared against the measured sediment transport. The results are expressed in terms of the discrepancy ratio (r) defined as the ratio of the predicted and measured transport rate. Table 5 shows the percentage of r values of the two data sets falling in the range of $0.5 \leqslant r \leqslant 2$. The table also summarizes results from the SEDTRANS96 model.

Based on the predictions by Sedtrans05, the methods of Van Rijn and Yalin yield the best results for SIB82 data with over 85% of the predicted transport rates within a factor of 2 of the measured values (Fig. 3E and D). In the case of medium sand (SIB93), the computed values according to Yalin and Van Rijn are too small at low transport stages and too large at higher transport stage. The SIB93 data set shows that the algorithms of Einstein–Brown and Bagnold give the best results with 64% and 62% of predicted values within a factor 2 of the measured values respectively (Fig. 3B and C). The Bagnold method tends to underestimate the transport rate for both medium and fine sand, whilst, on average, the computed values according to Einstein–Brown for fine sand are too small. The deviation is greatest for the Engelund–Hansen total load method (Fig. 3A).

For the current-dominated environment with very fine sand (Venice), the best predictions are given by the Van Rijn method and the Einstein–Brown method, with 76% and 67% of the predicted transport rates within a factor of 2 of the measured values, respectively. The methods of Yalin, Engelund–Hansen, and Bagnold overestimate the sediment transport. The method of Bagnold gives particularly bad results for these high transports of very fine sand by currents only.

The new version gives better estimations of the sediment-transport rate for fine sand (SIB82) than SEDTRANS96. The results for medium sand (SIB93) and for very fine sand with currents only (Venice) are as good as Sedtrans96. Differences in the Einstein–Brown computation between the two model versions are due to the Soulsby settling-velocity formulation (Soulsby, 1997) used in Sedtrans05.

Table 5
Validation of non-cohesive transport equations: percentage of predicted value (by SEDTRANS96 and Sedtrans05) within factor 2 of measured values

Method	SIB93, $D = 0.34$ mm		SIB82, $D = 0.20$ mm		Venice, $D = 0.11$ mm	
	SEDTRANS96 (%)	Sedtrans05 (%)	SEDTRANS96 (%)	Sedtrans05 (%)	SEDTRANS96 (%)	Sedtrans05 (%)
Engelund–Hansen (1967)	44	43	65	65	24	24
Einstein–Brown (1950)	64	62	62	54	67	67
Bagnold (1963)	64	64	38	42	5	5
Yalin (1963)	32	32	46	88	48	48
Van Rijn (1993)	–	47	–	85	–	76

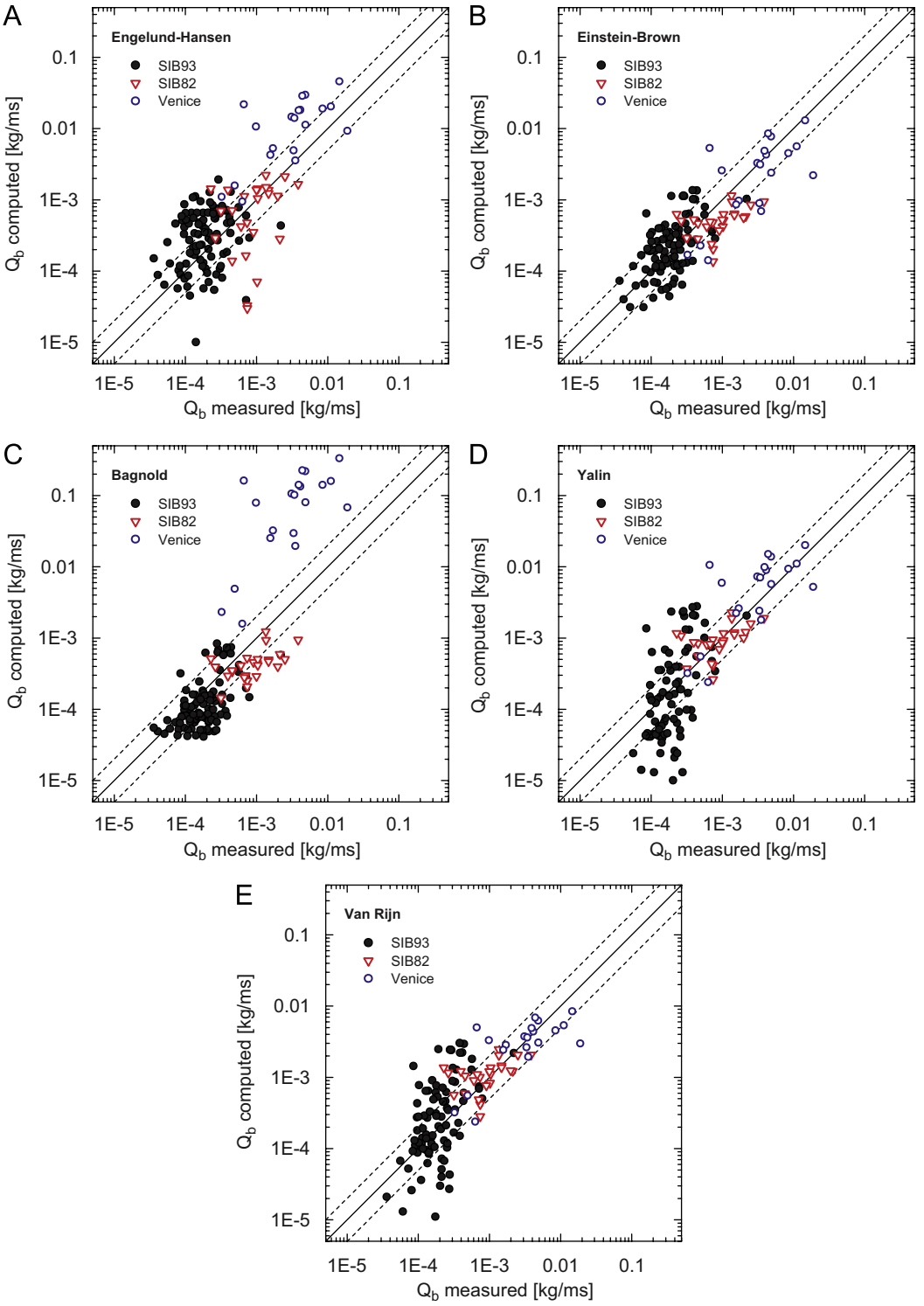

Fig. 3. A comparison between measured rates of sediment transport and rates computed according to the five non-cohesive transport equations in Sedtrans05. Solid dots are data from the 1993 deployment over medium sand (SIB93), triangles are data from the 1982 deployment over fine sand (SIB82), and open circles are data from Venice (2006). Solid line indicates perfect agreement; dashed lines represent factors 0.5 and 2.

5.2. Calibration of cohesive sediment algorithm

The cohesive algorithm of Sedtrans05 was calibrated with the data of field experiments with annular flumes. An annular flume is a closed system, which corresponds to a horizontal sediment bed with laterally invariable properties. A special interface to Sedtrans05 was written for the calibration, the 1D (vertical)-time model *SEDI1D*. τ_0 was preliminarily computed according to the specific flume calibration from current-meter data or lid-rotation speed. It was then used directly as an input parameter the subroutine COHESIVE.

The accuracy of the predicted SSC (SSC_{pred}) in comparison with the experimentally measured SSC (SSC_{meas}) is evaluated by calculating for each time step the proportional difference $PD = (SSC_{pred}/SSC_{meas} - 1)$. The overall fit of a predicted time series, σ_{PD}, is computed as the standard deviation of the proportional difference. The time percentage when the difference is less than 20% ($-0.2 > PD > 0.2$) is called $F_{20\%}$. Fig. 5 shows these statistical parameters computed for the interval from the start to the end of erosion.

The Sea Carousel and the submersible Mini Flume were deployed at several locations in Venice lagoon in February 1999 (Amos et al., 2004). Sedtrans05 reproduces correctly the erosion and the beginning of the settling of these field experiments (Figs. 4 and 5). The model produces a

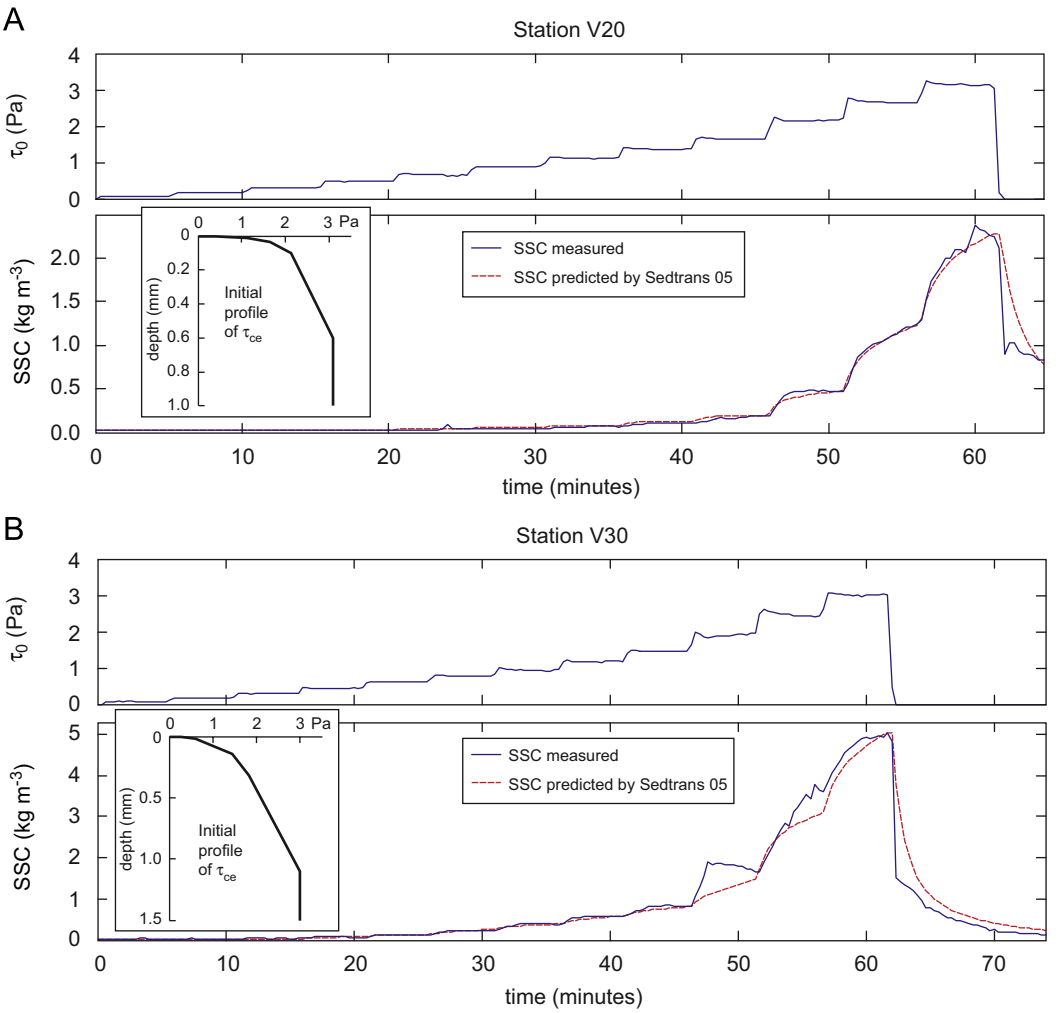

Fig. 4. A comparison of the cohesive sediment algorithm with field data collected with the Sea Carousel in Venice lagoon (Stations 20 and 30, February 1999). Initial profile of critical erosion threshold τ_{ce}, and time series of applied bed shear stress τ_0, measured SSC, and SSC predicted by Sedtrans05 are shown.

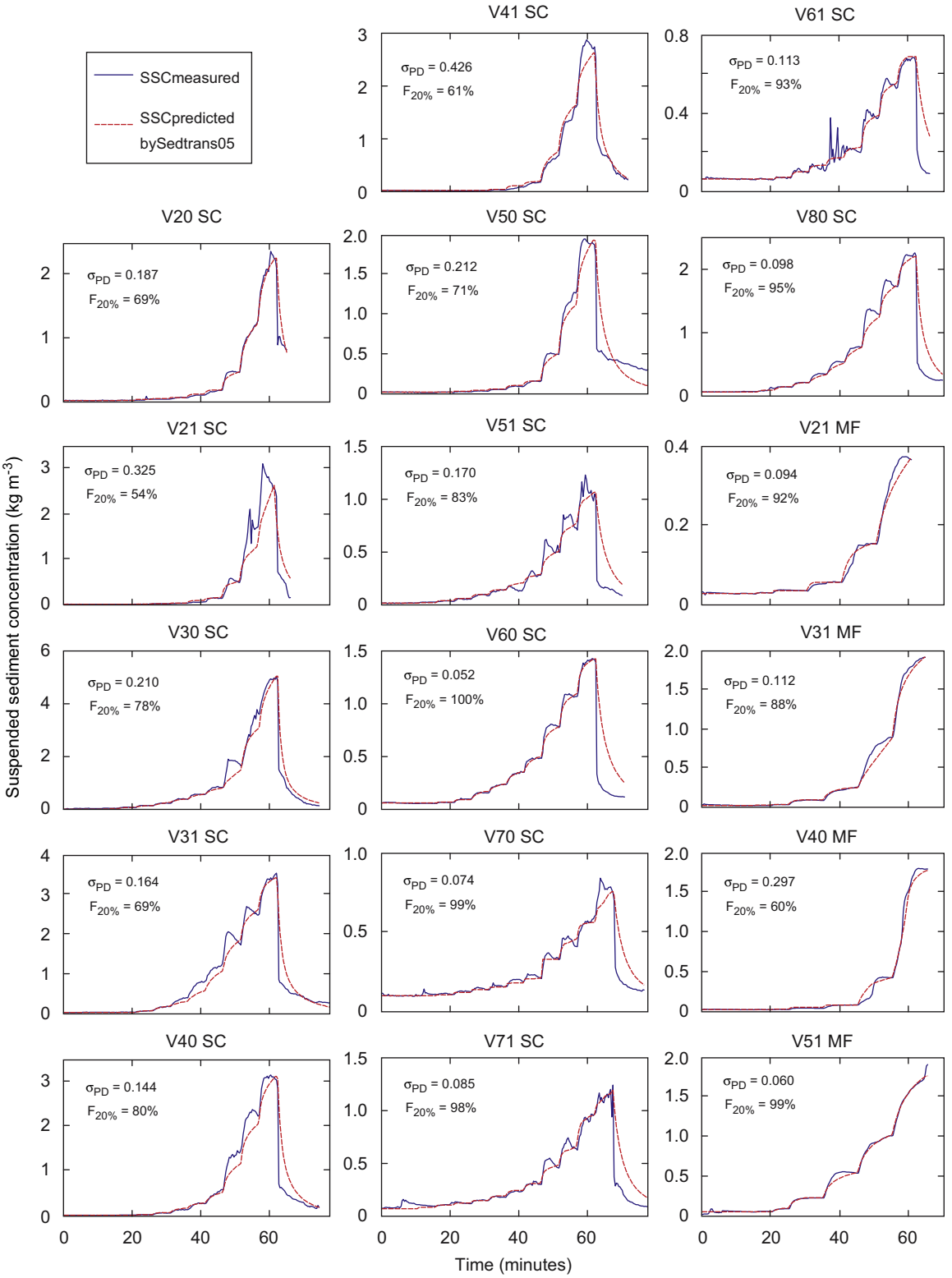

Fig. 5. A comparison of the cohesive sediment algorithm with field data collected with the Sea Carousel (SC) and the field Mini Flume (MF) at different stations in Venice lagoon, February 1999. For each experiment, time series of SSC measured and predicted by Sedtrans05, standard deviation of proportional difference (σ_{PD}), and time percentage when difference is less than 20% ($F_{20\%}$) are shown. See Fig. 4 for the pattern of applied bed shear stress during each experiment.

smoothed SSC curve that follows well the experimental erosion trends. The standard deviation of the proportional difference, σ_{PD}, is below 0.1 in 1/3 of the experiments, and below 0.2 in 3/4 of the experiments. However, the experimental data sometimes show irregularities (for example Fig. 4B) that cannot be explained through Eq. (12). Good model results require as input parameter initial characteristics of the bed for each specific experiment. In addition, the coefficients E_0 and P_e of Eq. (12) were customized for each field campaign (Table 4) to reproduce more accurately the erosion rates.

The settling part of the cohesive sediment algorithm worked well with generic input data, showing in detail the deposition of the different SSC fractions depending on τ_0. However, adequate experimental data are missing to calibrate in detail the settling part and the link between erosion process and SSC characteristics (Eqs. (13) and (14)).

6. Summary and conclusions

Sedtrans05 is the latest version of the sediment-transport model Sedtrans. The major modifications from the previous version are:

(a) The code is reorganized so that the calculation routines of Sedtrans05 can easily called from various programs. A console interface and a graphic user interface have been written, but it has also been linked with Matlab (with a dll Matlab function), with ArcView (with a dll), and with a 3D hydrodynamic model SHYFEM (Ferrarin et al., 2004).
(b) The Van Rijn (1993) method was added for non-cohesive sediment. It shows acceptable to good agreement with field data (Table 5), and it is recommended for a large grain-size range (Table 3).
(c) A new cohesive sediment algorithm models in detail variations of bed characteristics with depth, erosion, several classes of suspended sediment, flocculation, and deposition.

Sedtrans05 uses well-established calculation methods for non-cohesive sediment transport. However, it is important to select carefully the calculation methods. Some compute only bedload, others bedload and suspended load (Table 3). The physical approaches, the assumptions, and the ranges of calibration grain sizes differ in each case. The predicted transport rates between the methods vary up to a factor of 10.

A particular behaviour of Sedtrans05 was noticed during sensitivity analyses. The bedform prediction, which is based on fixed thresholds (Li and Amos, 1998), influences significantly the bed roughness. For this reason, the computed bed shear stress and the predicted transport rate may vary suddenly at the thresholds for bedform generation.

The new cohesive sediment algorithm reproduces several processes affecting cohesive sediment transport, but it does not include biostabilization and fluid mud transport. It does not compute the profile of SSC based on turbulence and settling; therefore it is adapted to relatively shallow water with a well-mixed water column. For deeper or more complex flows, a sediment diffusion model may be coupled with Sedtrans05 for more accurate prediction.

The calibration with field data shows that the cohesive sediment algorithm can predict correctly the erosion processes; however, detailed information on the bed characteristics is necessary. With a standard bed, the model predictions can be inaccurate because of the large variability in the erodability of natural sediments (Black et al., 2002). Additional research is needed to understand more fully the influence of biological activity, the consolidation history, and mineralogical composition on bed erosion. The deposition part of the model works well, but additional experimental data are required to calibrate the link between the erosion process and the characteristics of suspended sediment.

Acknowledgements

The present research was partially funded by the projects CORILA and EUROSTRATFORM. This paper is also a contribution of the Centre for Coastal Processes, Engineering and Management (CCPEM) of the University of Southampton. We thank Christopher Sherwood for his constructive review.

Appendix A. Command-line syntax of SED05

```
Command-line syntax for using the 1D version of Sedtrans05 (version 1.04)
SED05 [-b [INPUT-FILE [OUTPUT-FILE]]] [-o OUTPUT-FILE] [-c PARAMFILE] [-f] [-h] [-v]
     -b Batch mode with optionally names of input and output files
     (default is interactive mode)
     -o Specify the name of the output files
     -c Modify defaults parameters according to the file PARAMFILE
     -f Only one tabular output file for non-cohesive sediments
     -h No header line in tabular output files
     -v Input water density/dyn.viscosity instead of salinity/temperature
Special options:
SED05 -?            Show the present help text
SED05 -L            Show the licence
SED05 -e            Generate an example input-file 'INDATA.DAT' for batch-mode
                    runs, an example file 'INDATA.CST' to modify the default
                    parameters and write the list of abbreviations used in the
                    output files to the file 'OUTPUT.LST'
IN-FILE must be with extension, default IN-FILE (batch mode) is 'INDATA.DAT'.
OUT-FILE must be without extension, default OUT-FILE (batch and interactive modes)
is 'OUTPUT.*'.
Examples of usage:
        SED05                 Interactive mode with default output files
        SED05 -b cases.csv    Batch mode with input 'cases.csv' and output
                              'cases.*'
```

Appendix B. Supporting Information

Supplementary data associated with this article can be found in the online version at doi:10.1016/j.cageo.2008.02.007.

References

Amos, C.L., Daborn, G.R., Christian, H.A., Atkinson, A., Robertson, A., 1992. In situ erosion measurements on fine-grained sediments from the Bay of Fundy. Marine Geology 108, 175–196.

Amos, C.L., Cloutier, D., Cristante, S., Cappucci, S., Le Couturier, M., 2000. The Venice Lagoon Study (F-ECTS), Field Results, February 1999. Geological Survey of Canada Open File Report 3904, 220pp.

Amos, C.L., Bergamasco, A., Umgiesser, G., Cappucci, S., Cloutier, D., DeNat, L., Flindt, M., Bonardi, M., Cristante, S., 2004. The stability of tidal flats in Venice Lagoon—the results of in-situ measurements using two benthic, annular flumes. Journal of Marine Systems 51, 211–241.

Amos, C.L., Helsby, R., Lefebvre, A., Thompson, C.E.L., Villatoro, M., Venturini, V., Umgiesser, G., Zaggia, L., Mazzoldi, A., Tosi, L., Rizzetto, F., Brancolini, G., 2007. The origin and transport of sand in Venice lagoon, the latest developments. CORILA Special Publication, Venice, vol. 6, in press.

Andersen, T.J., Pejrup, M., 2002. Biological mediation of the settling velocity of bed material eroded from a intertidal mudflat, the Danish Wadden Sea. Estuarine, Coastal and Shelf Science 54, 737–745.

Bagnold, R.A., 1963. Mechanics of marine sedimentation. In: Hill, M.N. (Ed.), The Sea, vol. 3. Wiley-Interscience, New York, pp. 507–527.

Bagnold, R.A., 1966. An approach to the sediment transport problem from general physics. US Geological Survey Professional Paper 442-1, 37pp.

Bagnold, R.A., 1973. The nature of saltation and of "bed-load" transport in water. Proceedings of the Royal Society of London A 332, 473–504.

Best, J.L., Leeder, M.R., 1993. Drag reduction in turbulent muddy seawater flows and some sedimentary consequences. Sedimentology 40, 1129–1137.

Black, K.S., Tolhurst, T.J., Paterson, D.M., Hagerthey, S.E., 2002. Working with natural cohesive sediments. Journal of Hydraulic Engineering 128, 2–8.

Brown, C.B., 1950. Sediment transportation. In: Rouse, H. (Ed.), Engineering Hydraulics. Wiley, New York, pp. 769–857.

Cozette, P.M.F., 2000. Contribution of an alga (*Ulva*) to the erosion of cohesive sediments: towards the modelling of the phenomenon. M.Sc. Thesis, Department of Civil and

Environmental Engineering, University of Southampton, Southampton, Great Britain, 51pp.
Davidson, S., Amos, C.L., 1985. A re-evaluation of SED1D and SED2D: sediment transport models for the continental shelf. Geological Survey of Canada Open File Report 1705, Sect. 3, 54pp.
De Vries, M., Klaassen, G.J., Striksma, N., 1989. On the use of movable bed models for rivers problems: state of the art. In: Proceedings of the Symposium on River Sedimentation, Beijing, China.
Droppo, I.G., Lau, Y.L., Mitchell, C., 2001. The effect of depositional history on contaminated bed. Science of the Total Environment 266, 7–13.
Dyer, K.R., 1986. Coastal and Estuarine Sediment Dynamics. Wiley, Chichester, 342pp.
Dyer, K.R., Evans, E.M., 1989. Dynamics of turbidity maximum in a homogeneous tidal channel. Journal of Coastal Research, Special Issue 5, 23–30.
Engelund, F., Hansen, E., 1967. A Monograph on Sediment Transport in Alluvial Streams. Teknisk Vorlag, Copenhagen, 62pp.
Ferrarin, C., Neumeier, U., Umgiesser, G., Amos, C.L., 2004. Modelling the sediment transport in the Venice lagoon. In: Abstract at the congress: "EURODELTA-EUROSTRATA-FORM Annual Meeting," Venice, Italy.
Flindt, M.R., Neto, J., Amos, C.L., Pardal, M.A., Bergamasco, A., Pedersen, C.B., Andersen, F.Ø., 2004. Plant bound nutrient transport, mass transport in estuaries and lagoons. In: Nielsen, S.L., Banta, G.T., Pedersen, M.F. (Eds.), The Influence of Primary Producers on Estuarine Nutrient Cycling, the Fate of Nutrients and Biomass. Kluwer Academic Publishers, Dordrecht, pp. 93–128.
Fofonoff, N.P., 1985. Physical properties of seawater: a new salinity scale and equation of state for seawater. Journal of Geophysical Research 90, 3332–3342.
Gibbs, R.J., Matthews, M.D., Link, D.A., 1971. The relationship between sphere size and settling velocity. Journal of Sedimentary Petrology 41, 7–18.
Grant, W.D., Madsen, O.S., 1979. Combined wave and current interaction with a rough bottom. Journal of Geophysical Research 84, 1797–1808.
Grant, W.D., Madsen, O.S., 1986. The continental shelf bottom boundary layer. Annual Review of Fluid Mechanics 18, 265–305.
Harris, C.K., Wiberg, P.L., 2001. A two-dimensional, time dependent model of suspended sediment transport and bed reworking for continental shelves. Computer & Geosciences 27, 675–690.
Kranck, K., Milligan, T.G., 1992. Characteristics of suspended particles at an 11-hour anchor station in San Francisco Bay, California. Journal of Geophysical Research 97, 11373–11382.
Krone, R.B., 1993. Sedimentation revisited. In: Mehta, A.J. (Ed.), Nearshore and Estuarine Cohesive Sediment Transport. Coastal and Estuarine Studies 42. American Geophysical Union, Washington, DC, pp. 108–125.
Le Normant, C., 2000. Three-dimensional modelling of cohesive sediment transport in the Loire Estuary. Hydrological Processes 14, 2231–2243.
Lesser, G.R., Roelvink, J.A., van Kester, J.A.T.M., Stelling, G.S., 2004. Development and validation of a three-dimensional morphological model. Coastal Engineering 51, 883–915.
Li, M.Z., Amos, C.L., 1995. SEDTRANS92: a sediment transport model for continental shelves. Computer & Geosciences 21, 533–554.
Li, M.Z., Amos, C.L., 1998. Predicting ripple geometry and bed roughness under combined waves and currents in a continental shelf environment. Continental Shelf Research 18, 941–970.
Li, M.Z., Amos, C.L., 1999. Field observations of bedforms and sediment transport thresholds of fine sand under combined waves and currents. Marine Geology 158, 147–160.
Li, M.Z., Amos, C.L., 2001. SEDTRANS96: the upgraded and better calibrated sediment-transport model for continental shelves. Computers & Geosciences 27, 619–645.
Li, M.Z., Gust, G., 2000. Boundary layer dynamics and drag reduction in flows of high cohesive sediment suspensions. Sedimentology 47, 71–86.
Li, M.Z., Amos, C.L., Heffler, D.E., 1997. Boundary layer dynamics and sediment transport under storm and non-storm conditions on the Scotian Shelf. Marine Geology 141, 157–181.
Li, Z.H., Nguyen, K.D., Brun-Cottan, J.C., Martin, J.M., 1994. Numerical simulation of the turbidity maximum transport in the Gironde estuary (France). Oceanologica Acta 17, 479–500.
Martec Ltd., 1987. Upgrading of AGC sediment transport model: Geological Survey of Canada Open File Report 1705, Sect. 10, 14pp.
Mehta, A.J., 1988. Laboratory studies on cohesive sediment deposition and erosion. In: Dronkers, J., van Leussen, W. (Eds.), Physical Processes in Estuaries. Springer, Berlin, pp. 427–445.
Mehta, A.J., Lott, J.W., 1987. Sorting of fine sediment during deposition. In: Krauss, N.C. (Ed.), Coastal Sediment '87: Proceedings of a Speciality Conference on Advances in Understanding of Coastal Sediment Processes, vol. 1. American Society of Civil Engineers, New York, pp. 348–362.
Migniot, C., 1989. Tassement et rhéologie des vases, première partie (Bedding-down and rheology of muds, first part). Houille Blanche 44, 11–29.
Mulder, H.P.J., Udink, C., 1991. Modelling of cohesive sediment transport. A case study: the western Scheldt estuary. In: Edge, B.L. (Ed.), Proceedings of the 22nd International Conference on Coastal Engineering. American Society of Civil Engineers, New York, pp. 3012–3023.
Pane, V., Schiffman, R.L., 1985. A note on sedimentation and consolidation. Géotechnique 35, 69–72.
Pandoe, W.W., Edge, B.L., 2004. Cohesive sediment transport in the 3D hydrodynamic-baroclinic circulation model, study case for idealized tidal inlet. Ocean Engineering 31, 227–2252.
Parchure, T.M., Mehta, A.J., 1985. Erosion of soft cohesive sediment deposits. Journal of Hydraulic Engineering 111, 1308–1326.
Perkins, R.G., Sun, H., Watson, J., Player, M.A., Gust, G., Paterson, D.M., 2004. In-line laser holography and video analysis of eroded flocs from engineered and estuarine sediments. Environmental Science and Technology 38, 4640–4648.
Riley, J.P., Skirrow, G., 1965. Chemical Oceanography, vol. 3. Academic Press, London, 564pp.
Ross, M.A., Mehta, A.J., 1989. On the mechanics of lutoclines and fluid mud. Journal of Coastal Research 5, 51–62.

Sanchez, M., Grovel, A., 1994. Settlement: a sedimentary process. In: Bérogey, M., Rajaona, R.D., Sleath, J.F.A. (Eds.), Sediment Transport Mechanism in Coastal Environments and Rivers. EUROMECH 310. World Scientific, Singapore, pp. 146–151.

Sills, G.C., 1997. Consolidation of cohesive sediments in settling columns. In: Burt, N., Parker, R., Watts, J. (Eds.), Cohesive Sediments. Wiley, Chichester, pp. 107–120.

Smith, J.D., 1977. Modelling of sediment transport on continental shelves. In: Goldberg, E.D., McCave, I.N., O'Brien, J.J., Steele, J.H. (Eds.), The Sea, vol. 6. Wiley-Interscience, New York, pp. 539–576.

Soulsby, R.L., 1983. The bottom boundary layer of shelf seas. In: Johns, B. (Ed.), Physical Oceanography of Coastal and Shelf Seas. Elsevier Science Publishers, Amsterdam, pp. 189–266.

Soulsby, R., 1997. Dynamics of Marine Sands: A Manual for Practical Applications. Thomas Telford, London, 249pp.

Thompson, C.E.L., Amos, C.L., Jones, T.E.R., Chaplin, J., 2003. The manifestation of fluid-transmitted bed shear stress in a smooth annular flume—a comparison of methods. Journal of Coastal Research 19, 1094–1103.

Toorman, E.A., 1996. Sedimentation and self-weight consolidation: general unifying theory. Géotechnique 46, 103–113.

Umgiesser, G., 1997. Modelling the Venice Lagoon. International Journal of Salt Lake Research 6, 175–199.

Umgiesser, G., Depascalis, F., Ferrarin, C., Amos, C.L., 2006. A model of sand transport in Treporti channel: northern Venice lagoon. Ocean Dynamics 56, 339–351.

Van Rijn, L.C., 1993. Principle of Sediment Transport in Rivers, Estuaries and Coastal Seas. Aqua Publications, Amsterdam multiple pagination.

Whitehouse, R.J.S., Soulsby, R.L., Roberts, W., Mitchener, H.J., 2000. Dynamics of Estuarine Muds, A Manual for Practical Applications. Thomas Telford, London, 210pp.

Wiberg, P.L., Drake, D.E., Cacchione, D.A., 1994. Sediment resuspension and bed armouring during high bottom stress events on the northern California inner continental shelf: measurements and predictions. Continental Shelf Research 14, 1191–1219.

Winterwerp, J.C., van Kesteren, W.G.M., 2004. Introduction to the Physics of Cohesive Sediment in the Marine Environment. Developments in Sedimentology 56. Elsevier, Amsterdam, 559pp.

Yalin, M.S., 1963. An expression for bedload transportation. Journal of the Hydraulics Division, Proceedings of ASCE 89 (HY3), 221–250.